

# CO Adsorption on Thin MgO Films and Single Au Adatoms: A Scanning Tunneling Microscopy Study

Bing Yang,<sup>†,‡</sup> Xiao Lin,<sup>†</sup> Hong-Jun Gao,<sup>‡</sup> Niklas Nilus,<sup>\*,†</sup> and Hans-Joachim Freund<sup>†</sup>

Fritz-Haber-Institut der Max-Planck-Gesellschaft, Faradayweg 4-6, D-14195 Berlin, Germany, and Institute of Physics, Chinese Academy of Sciences, P.O. Box 603, Beijing 100190, China

Received: January 26, 2010; Revised Manuscript Received: April 8, 2010

The adsorption behavior of CO on a 2 ML thin MgO/Ag(001) film is investigated with scanning tunneling microscopy and spectroscopy at 5 K. Depending on the tip state, single CO molecules are imaged as Gaussian depressions or ring-like features on the oxide surface. The preferred CO adsorption sites are identified as the Mg<sup>2+</sup> positions next to an oxide step edge. The deposition of single Au atoms followed by CO exposure gives rise to the formation of monocarbonyl species on the MgO surface. Their vibrational properties are explored by inelastic electron-tunneling spectroscopy. The acquired second-derivative spectra are dominated by a symmetric peak/dip structure at  $\pm 50$  mV, which is assigned to the frustrated rotation of Au-bound CO molecules.

## 1. Introduction

Infrared reflection–absorption spectroscopy (IRAS) using CO as a probe molecule is one of the most common experimental techniques to characterize metal–oxide systems as used in catalysis.<sup>1,2</sup> The interpretation of the spectral data in terms of the CO binding site and the charge state of the local environment is usually based on theoretical approaches and experiments on structurally well-defined samples, for example, single crystals.<sup>3–6</sup> Such an assignment involves however a certain degree of uncertainty, given the complexity of real metal–oxide systems. Furthermore, the vibrational frequencies of CO are influenced by various, often opposing trends that are not easily elucidated from the IR data. For example, CO experiences a red-shift of its stretch frequency on strong binding sites, for example, defects, but also on negatively charged adatoms and clusters due to a filling of its antibonding CO  $2\pi^*$  orbital and the associated weakening of the intermolecular bond.<sup>7,8</sup> In contrast, a blue-shift is observed in weak binding configurations and electron-poor environments.<sup>9</sup> An identification of the CO binding characteristics only on the basis of IR absorption data is therefore ambiguous, and probing CO adsorption sites with a spatially resolving method would be highly desirable.

Scanning tunneling microscopy (STM) is in principle able to fulfill this requirement, as single CO molecules can be detected on the surface.<sup>10–12</sup> Moreover, inelastic electron-tunneling spectroscopy (IETS) provides a means to probe vibrational properties of the molecules and therefore enables a direct correlation with the IR data.<sup>13</sup> The potential of this method in analyzing the CO binding configuration has been demonstrated for various metal substrates.<sup>10,11,14</sup> Also, single metal carbonyls, synthesized by CO exposure to Fe, Pd, Ag, or Au adatoms, have been explored by STM.<sup>15–17</sup>

Unfortunately, the experiments on metal supports are not easily transferred to oxides, although the latter are more relevant for chemical applications. So far, only a single study for CO

on TiO<sub>2</sub>(110) has been reported in the literature.<sup>18</sup> The difficulties to probe CO on oxide surfaces are two-fold: (i) the CO binding energies are much smaller than on metal supports, and (ii) the required tip–surface distance to stabilize a preset current is shorter because of the lower sample conductivity. As a consequence, the CO easily desorbs under the tip influence, which hampers imaging and spectroscopy of CO on oxide materials.

This paper reports an STM study of the CO binding behavior on a pristine and a gold-covered MgO film grown on Ag(001). Nanosized gold on oxide supports has recently attracted much attention due to the unexpected catalytic activity of such systems in the low-temperature CO oxidation.<sup>19</sup> In addition, unusual CO adsorption properties have been reported for the Au–MgO system, that become manifest in an extremely low CO stretch frequency of 1850–1900 cm<sup>-1</sup> ( $\sim 235$  meV). The result was explained by a negative charging of Au on thin or highly defective MgO films<sup>7</sup> or alternatively by a strong polarization of the Au orbitals toward the CO on thicker ones.<sup>8</sup> Such peculiarities render the Au–MgO system an ideal test case to explore the adsorption of CO with an STM-based experiment.

## 2. Experiment

The experiments were carried out with a liquid-helium cooled ( $T = 5$  K), ultrahigh-vacuum STM.<sup>20</sup> The Ag(001) sample was cleaned by repeated cycles of Ar<sup>+</sup> sputtering (600 eV and 10  $\mu$ A) and annealing to 700 K. MgO films of 2 ML thickness were prepared by reactive Mg deposition at 500 K in an oxygen ambiance of  $1 \times 10^{-6}$  mbar. Single Au atoms were deposited from a high-purity Au wire (99.95%) wrapped around a tungsten filament directly onto the cryogenic sample held at 10 K. After deposition, Au monomers and few ultrasmall clusters were observed on the oxide surface.<sup>21,22</sup> Carbon monoxide was dosed by backfilling the chamber with  $1 \times 10^{-6}$  mbar CO for 5 min. However, only a tiny fraction of the molecules actually reached the sample surface, while the majority got frozen on the cold parts of the microscope during exposure. Spectral information on the adsorbed CO was obtained by detecting the second bias-derivative of the tunnel current ( $d^2I/dV^2$ ) with the lock-in

\* Corresponding author. E-mail: nilus@fhi-berlin.mpg.de. Phone (Fax): 0049-30-8413-4191 (4101).

<sup>†</sup>Fritz-Haber-Institut der Max-Planck-Gesellschaft.

<sup>‡</sup>Chinese Academy of Sciences.

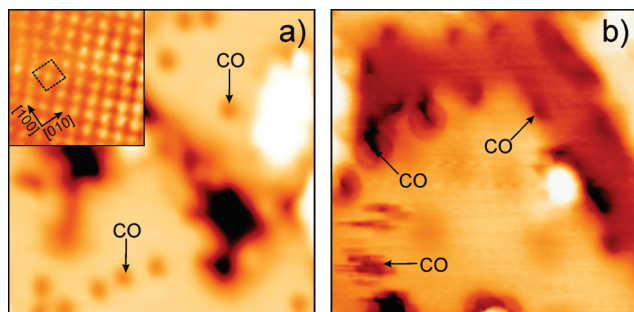


**Figure 1.** (a) STM topographic image of single CO molecules adsorbed on 2 ML MgO grown on Ag(001) ( $U_s = 0.1$  V,  $I = 3$  pA,  $11 \times 11$  nm<sup>2</sup>). The inset shows an atomically resolved image of the bare oxide film. (b) Similar STM image taken with a CO-modified tip ( $U_s = 0.3$  V,  $I = 3$  pA,  $7 \times 7$  nm<sup>2</sup>). Most of the molecules are found along the oxide step edges, whereby species at the upper step side appear as circular depressions due to interactions with the tip-bound CO. Molecules on the MgO terrace moved during the scan, giving rise to their streaky appearance.

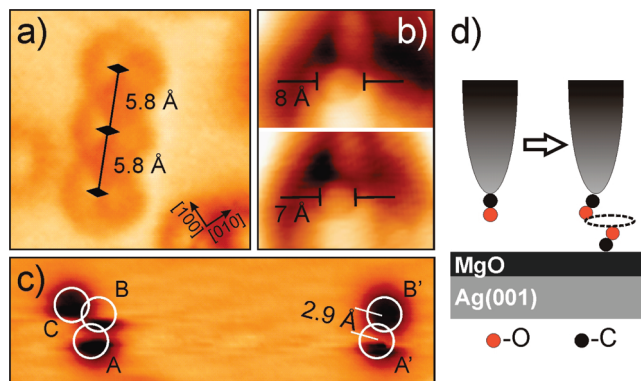
technique at 5 mV rms (root-mean-square) amplitude and 1 kHz modulation frequency.

### 3. Results and Discussion

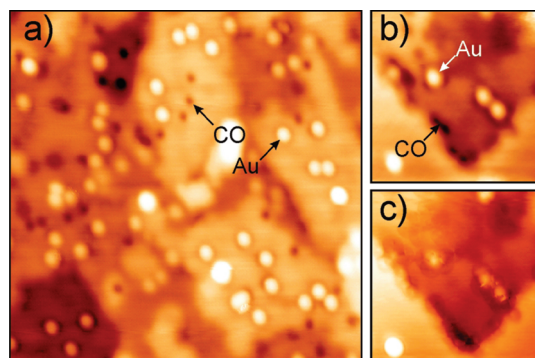
#### 3.1. CO Adsorption on the Bare MgO/Ag(001) Film.

Figure 1a shows a representative STM image of the 2 ML thick MgO/Ag(001) film after CO exposure. Three different oxide layers are exposed, their boundaries preferentially run along the nonpolar [100] directions. The contrast has been optimized for the second plane, rendering the first and third one mainly dark and white, respectively. With this contrast setting, several faint depressions are recognized on the oxide surface, which are assigned to single CO molecules (see arrows in Figure 1a). Their apparent height is determined to  $-0.25$  Å in low-bias STM images. A negative contrast for CO is commonly observed on metal surfaces and relates to the absence of molecular orbitals that support electron transport around the Fermi level ( $E_F$ ).<sup>10,23</sup> Only in a few cases, CO has been observed as protrusion, for example, on TiO<sub>2</sub>(110); however, the underlying contrast mechanism has not yet been elucidated.<sup>18</sup>

The STM measurement in Figure 1a was obtained with a metallic tip that imaged the CO as a simple Gaussian depression. Frequently, a CO got attached to the tip during scanning, reflecting the low binding strength of the molecule to the oxide surface. With such a modified tip, the CO molecules appeared as dark rings on the surface (Figures 1b and 2a).<sup>24</sup> The ring-like features might be explained by a repulsive interaction between the CO at the tip and the surface species. When the tip approaches the adsorbate, both molecules bend away from each other, and the tunnel current decreases (see sketch in Figure 2d). The current change is compensated by the STM feedback loop, and the tip approaches the surface within a circular region around the adsorbate. If tip and surface CO are directly above each other, further instabilities become visible, indicating a rapid movement of both molecules against each other. The resulting fuzzy contrast was used to identify the CO even on corrugated surfaces, where the regular CO-induced depressions could not be detected any more (Figure 1b). Indirect evidence for the proposed contrast mechanism came from STM images taken as a function of the tunnel current and tip-sample distance. The CO tilt angle and therefore the size of the ring structure on the surface were small at low currents but increased with higher currents due to the enhanced CO-CO repulsion (Figure 2b). Modified tips could be easily returned into a metallic state by applying a 2.0 V voltage pulse with open feedback loop.



**Figure 2.** (a) Topographic STM image of three CO molecules on 2 ML MgO/Ag(001), taken with a CO-covered tip ( $U_s = 0.1$  V, 3 pA). (b) Dependence of the CO-imaging characteristic on the tunnel current: upper panel  $I = 20$  pA, lower panel  $I = 3$  pA ( $U_s = -45$  mV). The diameter of CO-induced rings increases at higher current (smaller tip-sample distance) because of enhanced CO(tip)-CO(sample) interactions. (c) Tip-induced motion of two molecules on the oxide surface ( $U_s = 0.2$  V, 20 pA). The initial and final CO positions are marked by circles. (d) Sketch of CO(tip)-CO(sample) interaction that gives rise to the circular appearance of adsorbates in a and b.



**Figure 3.** (a) STM image of single Au atoms and CO molecules on MgO thin films ( $U_s = 0.1$  V, 3 pA,  $20 \times 20$  nm<sup>2</sup>). Topographic images of an identical surface region taken with (b) a metallic and (c) a CO-modified tip ( $U_s = 0.1$  V, 3 pA,  $7.7 \times 7.7$  nm<sup>2</sup>). Notice the fuzzy appearance of the Au species in c that indicates CO attachment to the adatoms.

Only the CO species on the oxide terraces are evident in Figure 1a, because the resolution was insufficient to probe step-bound molecules. However, the MgO step edges were actually identified as the preferred CO binding sites, as shown in Figures 1b and 3b. In the first image, CO molecules are found at the upper and lower side of a step edge. Whereas the up-step molecules are imaged as ring-like depressions, indicating a CO-covered tip, the down-step species appear as dark spots. The different appearance of both species might be explained by the limited degrees of freedom of CO molecules attached to a lower step side. Also in Figure 3b, the majority of CO is found along the low side of an MgO step edge, where it nearly agglomerates to a dark brim. To safely identify the dark holes as CO molecules, the tip was functionalized again with a CO to modify the image contrast. As expected, the depressions along the step edges adopted a characteristic fuzzy appearance due to the CO(tip)-CO(surface) interaction. The bright protrusions in Figure 3 are single Au atoms that will be discussed in the second part of this paper.

Only indirect conclusions could be drawn on the atomic binding site on the MgO film, as cations and anions were indistinguishable even in atomically resolved STM images (see inset of Figure 1a). However, CO clearly populates only a single

surface site, as measured CO–CO distances always correspond to multiples of the next-neighbor Mg–Mg (O–O) distance along the [110] and [100] direction of 2.9 and 4.2 Å, respectively. In general, next-neighbor sites were avoided, and the minimum distance between adjacent CO molecules was determined with 5.8 Å along the MgO[110] direction (Figure 2a). Similar information on the binding site was obtained from analyzing tip-mediated diffusion steps of CO molecules on the oxide surface. Stable imaging was achieved only with extremely soft tunnel conditions, namely, an electron current below 10 pA and a sample bias below 150 mV. A further increase of the tip–molecule interaction, for instance, due to modified imaging parameters or CO attachment to the tip, induced frequent jumps of the adsorbates on the oxide surface (Figure 1b, lower left). Figure 2c shows snapshots of such tip-induced diffusion steps of two CO molecules, being induced by scanning the tip from the bottom to the top. At the beginning, the CO molecules were located in sites A and A'. When the tip approached this region, they first jumped to B and B', and then the left molecule moved again to the C position. The jumps between A and B (A' and B') correspond to one next-neighbor distance between identical surface ions along the [110] direction (2.9 Å), while the B–C jump involved two adjacent sites along [1–10]. A careful analysis of several diffusion events revealed that CO jumps mainly occur between nearest-neighbor ions along the orthogonal MgO[110] directions and never comprise two nonequal surface sites, for example, a Mg<sup>2+</sup> and an O<sup>2-</sup> position.

The experimental results are in general agreement with the CO binding behavior on MgO(001) as determined by theory.<sup>25,26</sup> According to Hartree–Fock and density functional (DFT) calculations, the CO adsorbs with the C down to the surface Mg<sup>2+</sup> ions. The single binding site found in the experiments therefore corresponds to the cationic species. The interaction mainly results from an electrostatic attraction between the MgO Madelung field and the CO charge distribution and gives rise to adsorption energies of roughly 0.2 eV. This low binding strength is compatible with the mobile character of CO even at cryogenic temperatures. On step and corner sites of the MgO surface, the calculated binding energy rises to ~0.35 eV and ~0.58 eV, respectively, reflecting the higher electric field in the vicinity of low-coordinated surface sites.<sup>27,28</sup> Also this prediction is in perfect agreement with the experimental finding that most CO molecules attach to the MgO step edges. The observed CO adsorption at low-coordinated MgO sites therefore validates the interpretation of various thermal-desorption and vibrational studies in the literature.<sup>29,30</sup>

**3.2. CO Adsorption on Au Adatoms.** Figure 3 shows an STM topographic image of the MgO film after deposition of 0.01 ML Au and CO exposure at 5 K. The round and uniformly sized protrusions are easily identified as single Au adatoms (0.8 Å apparent height), while the larger features are small metal aggregates.<sup>21,22</sup> Furthermore, the same black dots as in Figure 1a are detected and assigned to CO molecules bound to the MgO terraces again. We expect that other molecules have interacted with the Au by forming monocarbonyl species on the surface. A direct distinction between Au atoms and Au–CO complexes was however not possible from the STM data, as neither the topographic height nor the conductance behavior of the adatoms changed in the accessible bias window ( $\pm 0.2$  V) upon CO exposure. In general, CO attachment modifies the STM appearance of metal atoms only if low-lying atomic orbitals are affected by the bond formation and the transport behavior of the junction is altered. Such an effect was revealed, for instance, for carbonyl species on FeO(111) and NiAl(110),

where the CO removes the Au 6s orbital from a region around  $E_F$  and triggers a reduction of the AuCO apparent height with respect to an Au atom.<sup>17,31</sup> For Au atoms on the MgO film, on the other hand, the Au 6s orbital is not involved in the electron transport, as the state is spatially confined and localized well below  $E_F$ .<sup>32</sup> Consequently, no change in the image contrast is observed after forming the Au–CO bond. Indirect evidence for the presence of carbonyl species is however revealed from STM images taken with a CO-covered tip. As discussed before, the CO(tip)–CO(sample) interaction leads to a blurred appearance of CO-containing surface species. Such an imaging characteristic is indeed visible in Figure 3c, which has been taken with a functionalized tip. Apparently, not only the oxide-bound CO but also the Au atoms exhibit a fuzzy contrast, indicating the presence of an attached CO molecule.

It should be noted that the computed CO binding energy to Au atoms on the MgO/Ag film is with 0.21 eV of the same order as for CO on the bare film.<sup>33</sup> This unusually weak bonding relates to the anionic nature of Au that results from a charge transfer out of the metal support through the ultrathin film.<sup>32</sup> The extra electron gives rise to a large Coulomb repulsion with the CO 5 $\sigma$  orbital, which drastically reduces the Au–CO interaction. In contrast, the Au–CO adsorption energy increases to 0.81 eV on thick MgO films where the Au atoms remain neutral.<sup>34</sup>

**3.3. Vibrational Spectroscopy of CO Molecules on Au/MgO.** The ultimate proof for the presence of CO on the MgO thin film would come from a vibrational identification of the molecules. The STM is in principle capable to detect vibrational modes of single molecules, exploiting the inelastic transport characteristics of electrons through the STM junction.<sup>13</sup> The excitation of molecular vibrations opens an additional transport channel for the tunneling electrons, which gives rise to a step in the differential conductance at the vibrational threshold. Usually, the second bias-derivative of the tunnel current ( $d^2I/dV^2$ ) is probed to enhance the visibility of the often tiny conductance change. In such  $d^2I/dV^2$  spectra, a characteristic peak/dip structure emerges at the positive/negative bias position of the vibrational mode. The symmetry of the feature with respect to  $E_F$  hereby reflects similar excitation cross sections of vibrational modes for electron tunneling into and out of the sample. IETS has proven its capacity to probe the vibrational signature of CO on different metal surfaces.<sup>14,15,17</sup> On oxide supports, only a modified IETS technique was realized so far, in which vibronic excitations were detected as a fine-structure superimposed onto the conductance behavior of a molecular orbital.<sup>35</sup> Classical IETS that detects energy losses around  $E_F$  has not been reported for CO or any other molecule on an oxide surface.

Figure 4a shows second-derivative spectra taken on the bare MgO film, a CO molecule, and an AuCO complex in the bias range of the frustrated CO vibrations. Although the spectra have similar shapes at first glance, tiny differences become visible when subtracting an MgO background from the AuCO spectra. In the difference spectrum, a symmetric peak/dip structure becomes visible at  $\pm (50 \pm 5)$  mV, having a full-width at half-maximum of 18 mV. The width is governed by the large bias modulation of 5 mV that was required to detect the features. The symmetry with respect to  $E_F$  suggests that the  $d^2I/dV^2$  feature is caused by a vibrational mode of the gold carbonyl. A similar, though weaker, peak/dip structure was revealed for oxide-bound CO molecules as well. To probe the spatial localization of the vibronic mode, second-derivative maps have been taken at around 50 mV (Figure 4b). An enhanced  $d^2I/dV^2$  contrast is

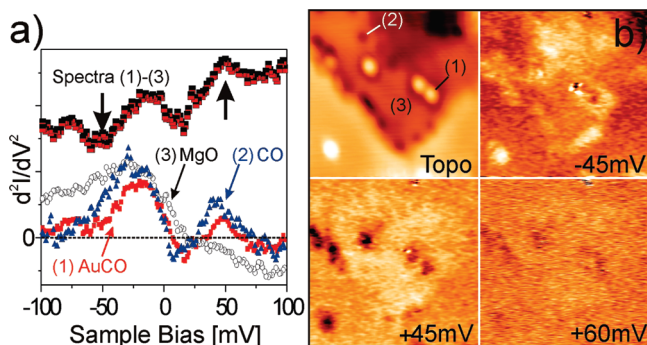


**Figure 4.** (a)  $d^2I/dV^2$  spectra taken on the bare MgO surface, a single CO molecule, and an AuCO species (set-point: 75 mV, 10 pA). The upper curve is the difference between the AuCO and the MgO spectra. The symmetric peak/dip structure at 50 mV is assigned to a vibrational excitation. The probed surface species are indicated in panel b. (b) Topographic and second-derivative images of CO and AuCO species on 2 ML MgO/Ag(001) (10 pA,  $7.7 \times 7.7 \text{ nm}^2$ ). The upper right and lower left maps have been taken close to the bias position of the peak/dip structure in a. The lower right map is measured at higher bias and shows no  $d^2I/dV^2$  contrast.

indeed observed at the AuCO positions, although also the step-bound CO molecules appear somewhat brighter. As expected, the contrast reverses in  $d^2I/dV^2$  maps taken at the dip position in the spectrum. The IETS intensity vanishes in  $d^2I/dV^2$  maps taken away from the CO vibrational modes (e.g., at 60 mV). This data set clearly demonstrates the confinement of the inelastic excitation in space and energy.

The AuCO vibration is assigned with the help of other experimental data and DFT calculations. On a NiAl(110) surface, a similar IETS feature at  $\pm 35$  mV has been related to the hindered rotation of CO in a gold carbonyl.<sup>17</sup> This particular mode is also the one with the highest excitation cross section of all CO modes in an STM-IETS experiment.<sup>36</sup> The blue shift of the CO hindered rotation in our case is compatible with the anionic character of Au atoms on the MgO thin film,<sup>32</sup> which shifts the frustrated modes to higher and the stretch modes to lower frequencies.<sup>7</sup> Mutual interactions between energetically close CO vibrations might contribute to the observed shift. DFT finds the frustrated rotation of single AuCO species on 2 ML MgO/Ag(001) at 40 meV, while adjacent modes are the external Au-CO stretch at 20.7 meV and the frustrated translation at 4 meV.<sup>37</sup> The best agreement with the experimental data is again obtained for the Au-CO frustrated rotation.

It needs to be emphasized that the identification of vibrational modes with the STM is not unambiguous for AuCO complexes on the MgO film. First, the  $d^2I/dV^2$  fingerprint of the carbonyls is extremely weak with respect to signals obtained on metal surfaces. The reason might be the large MgO band gap and the corresponding absence of final states for inelastic electrons in the oxide at  $E_F$ . Secondly, isotope-exchange experiments to verify a vibrational origin of the peak/dip structure failed because of the large width of the spectral features with respect to the expected peak shift. Thirdly, the CO stretch mode at  $\sim 235$  meV could not be probed, as the CO species immediately desorbed from the surface at this bias. The experiments therefore leave some open points in the vibrational characterization of CO molecules on the Au-MgO surface.

#### 4. Conclusion

The binding behavior of CO molecules to a 2 ML MgO film on Ag(001) and single Au adatoms has been investigated with STM. Step edges in the oxide surface are identified as the

preferred CO adsorption sites, although a few terrace-bound molecules are observed as well. CO attachment to single Au atoms is suggested from images taken with a CO-covered tip, which gives rise to a fuzzy contrast of the carbonyl species due to CO(tip)-CO(surface) interactions. IET spectra taken on the AuCO complexes reveal a symmetric peak/dip structure at  $\pm 50$  mV that is assigned to the frustrated rotation of the Au-bound CO molecule. The blue shift of this vibrational mode with respect to AuCO on metal surfaces is compatible with the negative charging of Au atoms on the thin MgO/Ag(001) films. Our study demonstrates that STM is a powerful technique to investigate the binding properties of small inorganic molecules even on an oxide surface.

**Acknowledgment.** The authors are grateful to Gianfranco Pacchioni for valuable discussion. X.L. thanks the Humboldt foundation. We acknowledge support from the Cluster of Excellence (UNICAT) funded by the Deutsche Forschungsgemeinschaft and coordinated by the Technische Universität Berlin.

#### References and Notes

- Freund, H. J.; Kühlenbeck, H.; Staemmler, V. *Rep. Prog. Phys.* **1996**, *59*, 283–347.
- Bäumer, M.; Freund, H. J. *Prog. Surf. Sci.* **1999**, *61*, 127–198.
- Hollins, P. *Surf. Sci. Rep.* **1992**, *16*, 51–94.
- Zecchina, A.; Scarano, D.; Bordiga, S.; Ricchiardi, G.; Spoto, G.; Geobaldo, F. *Catal. Today* **1996**, *27*, 403–435.
- Abbet, S.; Riedo, E.; Brune, H.; Heiz, U.; Ferrari, A.; Giordano, L.; Pacchioni, G. *J. Am. Chem. Soc.* **2001**, *123*, 6172.
- Meyer, R.; Lemire, C.; Shaikhutdinov, S.; Freund, H.-J. *Gold Bull.* **2004**, *37*, 72–124. Lemire, C.; Meyer, R.; Shaikhutdinov, S.; Freund, H.-J. *Angew. Chem., Int. Ed.* **2004**, *43*, 118–121.
- Sterrer, M.; Yulikov, M.; Fischbach, E.; Heyde, M.; Rust, H.-P.; Pacchioni, G.; Risse, T.; Freund, H.-J. *Angew. Chem., Int. Ed.* **2006**, *45*, 2630–2632.
- Sterrer, M.; Yulikov, M.; Risse, T.; Freund, H.-J.; Carrasco, J.; Illas, F.; Di Valentin, C.; Giordano, L.; Pacchioni, G. *Angew. Chem., Int. Ed.* **2006**, *45*, 2633–2635.
- Vindigni, F.; Manzoli, M.; Chiorino, A.; Boccuzzi, F. *Gold Bull.* **2009**, *42*, 106–112.
- Döring, M.; Buisset, J.; Rust, H. P.; Briner, B. G.; Bradshaw, A. M. *Discuss. Faraday Soc.* **1996**, *105*, 163–175.
- Bartels, L.; Meyer, G.; Rieder, K. H. *Chem. Phys. Lett.* **1998**, *297*, 287–292.
- Nilius, N.; Wallis, T. M.; Ho, W. *Phys. Rev. Lett.* **2003**, *90*, 1–4, 186102.
- Stipe, B. C.; Rezaei, M. A.; Ho, W. *Science* **1998**, *280*, 1732–1735.
- Lauhon, L. J.; Ho, W. *Phys. Rev. B* **1999**, *60*, R8525–R8528.
- Lee, H. J.; Ho, W. *Science* **1999**, *286*, 1719–1722.
- Nilius, N.; Wallis, T. M.; Ho, W. *J. Chem. Phys.* **2002**, *117*, 10947–10952.
- Wallis, T. M.; Nilius, N.; Ho, W. *J. Chem. Phys.* **2003**, *119*, 2296–2300.
- Zhao, Y.; Wang, Z.; Cui, X. F.; Huang, T.; Wang, B.; Luo, Y.; Yang, J. L.; Hou, J. G. *J. Am. Chem. Soc.* **2009**, *131*, 7958–7959.
- Haruta, M.; Yamada, N.; Kobayashi, T.; Iijima, S. *J. Catal.* **1989**, *115*, 301.
- Rust, H.-P.; Buisset, J.; Schweizer, E. K.; Cramer, L. *Rev. Sci. Instrum.* **1997**, *68*, 129–132.
- Sterrer, M.; Risse, T.; Pozzoni, U. M.; Giordano, L.; Heyde, M.; Rust, H.-P.; Pacchioni, G.; Freund, H.-J. *Phys. Rev. Lett.* **2007**, *98*, 096107.
- Simic-Milosevic, V.; Heyde, M.; Lin, X.; König, T.; Rust, H.-P.; Sterrer, M.; Risse, T.; Nilius, N.; Freund, H.-J.; Giordano, L.; Pacchioni, G. *Phys. Rev. B* **2008**, *78*, 235429.
- Kulawik, M.; Rust, H.-P.; Nilius, N.; Heyde, M.; Freund, H.-J. *Phys. Rev. B* **2005**, *71*, 153405.
- Bartels, L.; Meyer, G.; Rieder, K.-H. *Appl. Phys. Lett.* **1997**, *71*, 213–217. Nieminen, J. A.; Niemi, E.; Rieder, K.-H. *Surf. Sci.* **2004**, *552*, L47–L52.
- Pacchioni, G.; Cogliandro, C.; Bagus, P. S. *Surf. Sci.* **1991**, *255*, 344. Pacchioni, G.; Cogliandro, C.; Bagus, P. S. *Int. J. Quantum Chem.* **1991**, *42*, 1115.
- Pacchioni, G. *Surf. Rev. Lett.* **2000**, *7*, 277.

- (27) Pacchioni, G.; Minerva, T.; Bagus, P. S. *Surf. Sci.* **1992**, 275, 450.
- (28) Xu, Y.; Li, J.; Zhang, Y.; Chen, W. *Surf. Sci.* **2003**, 525, 13.
- (29) Wichtendahl, R.; Rodriguez-Rodrigo, M.; Härtel, U.; Kuhlenbeck, H.; Freund, H.-J. *Phys. Status Solidi A* **1999**, 173, 93.
- (30) Dohnalek, Z.; Kimmel, G. A.; Joyce, S. A.; Ayotte, P.; Smith, R. S.; Kay, B. D. *J. Phys. Chem.* **2001**, 105, 3747.
- (31) Rienks, E. D. L.; Nilius, N.; Freund, H.-J.; Giordano, L.; Pacchioni, G.; Goniakowski, J. *Phys. Rev. B* **2009**, 79, 075427.
- (32) Pacchioni, G.; Giordano, L.; Baistrocchi, M. *Phys. Rev. Lett.* **2005**, 94, 226104-1-4.
- (33) Giordano, L.; Martinez, U.; Sicolo, S.; Pacchioni, G. *J. Chem. Phys.* **2007**, 127, 144713.
- (34) Giordano, L.; Carrasco, J.; Di Valenti, C.; Illas, F.; Pacchioni, G. *J. Chem. Phys.* **2006**, 124, 174709-1-8.
- (35) Ogawa, N.; Mikaelian, G.; Ho, W. *Phys. Rev. Lett.* **2007**, 98, 166103-1-4.
- (36) Ho, W. *J. Chem. Phys.* **2002**, 117, 11033-11061.
- (37) Pacchioni, G. Dipartimento di Scienza dei Materiali, Università di Milano-Bicocca, 20125 Milano, Italy, private communication from Dec. 4, 2008.

JP100757Y